Journal Pre-proof

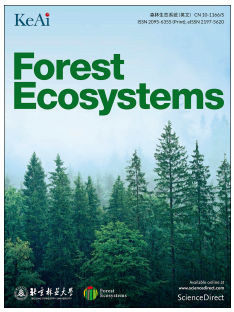

The overlooked role of individual variability in autumn xylem phenology and carbon sequestration

Chunsong Wang, Jean-Daniel Sylvain, Roberto Silvestro, Guillaume Drolet, Keyan Fang, Sergio Rossi

PII: S2197-5620(25)00123-X

DOI: https://doi.org/10.1016/j.fecs.2025.100414

Reference: FECS 100414

To appear in: *Forest Ecosystems*

Received Date: 10 August 2025

Revised Date: 18 November 2025

Accepted Date: 26 November 2025

Please cite this article as: Wang, C., Sylvain, J.-D., Silvestro, R., Drolet, G., Fang, K., Rossi, S., The overlooked role of individual variability in autumn xylem phenology and carbon sequestration, *Forest Ecosystems*, https://doi.org/10.1016/j.fecs.2025.100414.

The overlooked role of individual variability in autumn xylem phenology and carbon sequestration

Chunsong Wang[1,2], Jean-Daniel Sylvain[3,4], Roberto Silvestro[2], Guillaume Drolet[3], Keyan Fang[1,*], Sergio Rossi[2]

[1]Key Laboratory of Humid Subtropical Eco-Geographical Process (Ministry of Education), College of Geographical Sciences, Fujian Normal University, Fuzhou 350007, China

[2]Département des Sciences Fondamentales, Université du Québec à Chicoutimi, 555, boulevard de l'Université Chicoutimi, Chicoutimi, QC, G7H2B1, Canada

[3]Direction de la recherche forestière, ministère des Ressources naturelles et des Forêts, 2700, rue Einstein, Québec, QC, G1P3W8, Canada

[4]Hydrology, Climate and Climate Change Laboratory, École de technologie supérieure, Université du Québec, 1100 R. Notre Dame O, Montréal, H3C1K3, Canada

E-mail address: kfang@fjnu.edu.cn (K. Fang)

Abstract

Accurate modeling of carbon sequestration by forests requires scaling wood formation processes from trees to the landscape. The quantification of growth and carbon dynamics requires deep knowledge of the variability in xylem phenology among individuals. This study presents a comprehensive assessment of seasonal and individual variability in xylem phenology based on more than 800 balsam firs (*Abies balsamea* (L.) Mill.) monitored weekly across 33 plots from 2018 to 2022 in Montmorency Forest, Quebec, Canada. Wood microcores were collected from April to October to quantify the timings of cambial activity and xylem development on anatomical sections observed at high magnification under the microscope. The first enlarging cells appeared between late May and early June (day of the year (DOY) 153–167), and cell-wall thickening ended in late August (DOY 223–238), resulting in a growing season of 63 to 79 days. Xylem production ranged from 27.4 to 47.9 radial cells. While the onset of xylogenesis was well synchronized among individuals, within 2 weeks, the cessation of growth showed a greater variability, reaching up to 3 weeks. This autumnal variability was positively correlated with wood production, as higher cambial activity increases the accumulation of xylem cells to be differentiated. Our findings provide empirical evidence that individual variability in growth cessation reflects the underlying heterogeneity in cambial activity among trees of the same stand. Our results demonstrate the role of xylem phenology, especially during the autumn, in shaping forest growth. The assessment of both seasonal and individual variability in phenology is an essential step to improve the representation of autumn processes in forest carbon models, which can help to reduce the uncertainty in predictions of boreal forest growth under current or future climate scenarios.

Keywords: Xylogenesis; Cell production; Cell differentiation; Microcore; Sample size; *Abies balsamea*

1 Introduction

Forests are the largest terrestrial carbon sink, absorbing about 30% of the global annual CO_2 emissions, and play a key role in mitigating climate change (IPCC, 2023; FAO, 2022). Their ability to sequester carbon is strongly influenced by the seasonal dynamics of tree growth, particularly phenology, which governs the timings and duration of carbon uptake (Silvestro et al., 2024; Piao et al., 2019; Keenan et al., 2014). Climate-driven shifts in phenology, especially the earlier budburst in spring or delayed photosynthesis in autumn, can affect the annual carbon balance of forest ecosystems (Liu et al., 2025; Rossi et al., 2016; Richardson et al., 2013). Understanding these changes is essential for predicting how forests respond to climate change and how much carbon is ultimately stored in woody biomass. Most existing studies on tree phenology rely on leaf-based metrics, such as budburst and senescence, obtained through direct observations or remote sensing (Campioli et al., 2024; Piao et al., 2019; Fu et al., 2019; Gallinat et al., 2015). Despite their wide use and application, these metrics are particularly limited in autumn due to the gradual and species-specific nature of leaf senescence (Silvestro et al., 2025; Gallinat et al., 2015). The occurrence of multiple drivers of autumnal phenology introduces uncertainty in defining the end of the growing season, limiting our ability to disentangle the processes of carbon sequestration and carbon allocation, to assess forest productivity under changing climates, and to identify the major causes affecting the seasonal dynamics of tree growth.

Xylem phenology describes the phases of wood formation, i.e., cell division and differentiation, which are critical to assess carbon sequestration of forests. This process is typically monitored using high-resolution microcore sampling that enables accurate detection of cambial activity and development of xylem cells (Rossi et al., 2006a). Xylem phenology determines the length of the growing season, a key factor influencing carbon allocation into wood biomass (Silvestro et al., 2023; Keenan et al., 2014). The recent literature suggests that cambial reactivation is primarily driven by thermal signals, in the form of either threshold or accumulated heat (Zhang et al., 2024; Li et al., 2017; Rossi et al., 2016). In contrast, the cessation of wood formation seems to be

influenced by a more complex set of endogenous and environmental factors occurring in autumn, including photoperiod, weather, and the physiological status of the trees (Mu et al., 2023; Perrin et al., 2017; Gallinat et al., 2015). Because of this wide interaction of environmental and endogenous factors, autumn phenology exhibits a greater individual variability compared to the thermally-driven growth reactivation in spring (Rathgeber et al., 2011). There is an urgent need to analyze more deeply the individual variability in growth dynamics by proposing a systematic quantitative assessment of this seasonal contrast between spring and autumnal phenology.

The phenological variability among individuals involves trees with either early growth cessation or xylem formation extended later in autumn. Such a variability influences the statistical precision and accuracy of our estimations of the timings and amount of carbon assimilation of a stand (Marchand et al., 2020). Beyond its methodological implications, phenological asynchrony may also influence stand-level growth dynamics. If individual trees stagger their growth cessation, this temporal spread could reduce peak competition for resources within the stand and promote more efficient resource use (Rathgeber et al., 2011). As a result, cumulative wood production may increase when growth activity is distributed over a longer period (Rossi et al., 2016; Cuny et al., 2012). The relationship between the individual variability in phenology and wood growth is raising interest among forest ecologists. Phenological heterogeneity is a common feature of natural populations, and its potential impact in shaping growth dynamics and carbon sequestration has recently been investigated (Silvestro et al., 2025; Marchand et al., 2020; Delpierre et al., 2016). However, despite the growing interest in individual phenological variability, direct evidence linking variability in autumn phenology to xylem cell production is still limited.

Most studies on xylem phenology have been based on small sample sizes and short observation periods (Wang et al., 2023; X. Liu et al., 2019), raising concerns about the representativeness of their findings and the robustness of the statistics at the stand level. Although Silvestro et al. (2022) proposed sample size guidelines based on phenological data, the results were limited to a single year. A question remains on how much such

104 differences between spring and autumn phenology are stable in time. If autumn
105 phenology indeed exhibits higher individual variability as suggested, accurate
106 assessment at the population level may require larger sample sizes. Despite its relevance
107 for the accuracy of phenological analyses, this methodological aspect has received little
108 attention in the literature, potentially affecting the interpretation of seasonal growth
109 dynamics in trees.

110 To fill these gaps, we investigated the seasonal dynamics of xylem phenology using
111 balsam fir (*Abies balsamea* (L.) Mill.) as a model species, given its ecological
112 dominance and economic relevance in northeastern North America. Leveraging one of
113 the largest monitoring of intra-annual wood formation worldwide, involving a sample
114 of more than 800 trees in five years, we provide the first quantitative assessment of
115 individual variability in spring and autumn phenology. We conducted weekly microcore
116 sampling across 33 plots located in the same study area to track the timing of wood
117 formation during 2018–2022, enabling a robust evaluation of individual seasonal
118 variability and its implications for wood productivity. We tested two hypotheses related
119 to the variability in xylem phenology among individuals: 1) autumn has a greater
120 variability than spring; 2) a higher variability in autumn phenology corresponds to a
121 larger variability in xylem cell production.

122

2 Materials and methods

2.1 Study area

This study was conducted at the Montmorency Forest (47.32° N, 71.15° W, 850 m a.s.l.), located in the southern interior of Quebec, Canada. The local climate is shaped by both polar air masses and the North Atlantic Ocean, resulting in a typical boreal continental regime (He et al., 2025; Perrin et al., 2017). The growing season is short and mild, and the winter is long and cold. The mean annual temperature in the last 20 years was 0.9 °C. January is the coldest month with a mean temperature of −14.4 °C, and July is the warmest with a mean temperature of 15.0 °C. Total precipitation is 1,379 mm, of which 738 mm falls in the form of rain. Snow persists on the soil from the end of October to mid-May (Fig. 1). The climate is primarily limited by energy input, while the local variability in soil water content is significantly influenced by topography, soil properties, drainage regimes, and vegetation structure and type (Lagueux et al., 2024; Harel et al., 2023). The area belongs to the balsam fir–white birch bioclimatic domain (Lagueux et al., 2024), with balsam fir representing 80% of the stand composition.

2.2 Tree selection and sampling

A total of 33 plots (20 m × 20 m) were established within an area of 1 km^2. Four to five healthy and upright firs were selected annually per plot and sampled throughout the growing season (Fig. 1). Overall, more than 800 firs were selected for the weekly sampling throughout the study period. The selected trees had a diameter at breast height (DBH) of 11.8 ± 2.5 cm, a height of 9.3 ± 1.7 m (mean ± standard deviation (s.d.)), and an estimated age ranging from 25 to 35 years. Weekly microcores were collected from these trees during April-October from 2018 to 2022. Sampling was carried out at 1 to 2 m above ground using Trephor (Rossi et al., 2006a). Each microcore was 2 mm in diameter and 2–3 cm in length, and included at least two intact tree rings and the adjacent phloem tissue.

2.3 Lab analysis and data collection

The microcores were dehydrated through a graded alcohol series, cleared with limonene, and embedded in paraffin. Transverse sections (8 μm thick) were obtained using a rotary microtome, stained with cresyl violet acetate (Rossi et al., 2006b), and examined under both visible and polarized light at 250× magnification to distinguish xylem cells at different developmental phases along three rows per section. Cambial cells appeared as flattened cells with thin walls, enlarging cells showed larger sizes with irregular diameters, and wall-thickening cells exhibited birefringence under polarized light. Mature cells had fully developed secondary walls under polarized light (Rossi et al., 2006a, b). The number of cells in each section was averaged for each sample and developmental phase and associated to the corresponding DOY. The number of cells was interpolated between two successive observations on a daily basis using linear interpolation (Rossi et al., 2006b). The onset and ending of each developmental phase (cell enlargement, wall thickening and lignification, and maturation) were identified for every tree and determined as the DOY when the first or last tracheid was observed in each phase. Spring and autumn phenology refers to the onset (i.e., first enlarging, first wall thickening, and first mature cells) and cessation (i.e., ending of cell enlargement and ending of wall thickening) of xylogenesis.

2.4 Data analysis and statistics

Cell production was fitted by Gompertz functions (Rossi et al., 2006b) using Eq. 1:

$$y = \alpha e^{-e^{\beta-\kappa T}} \quad (1)$$

where y is the cell production, α is the upper asymptote, β is the *x*-axis placement parameter, κ is the rate of change, and T is the time, expressed as DOY.

We used a variance component analysis in mixed models to quantify the sources of variation in xylem phenology and cell production across hierarchical levels (i.e., temperature, precipitation, plot, and DBH). The relationships between phenological

events and their variability were analyzed using Pearson correlation and Mantel tests (Legendre et al., 2015). The relationship between phenological timing and duration was tested using sample linear regression, while the relationship between growth duration and cell production was assessed via standardized major axis (SMA) regression, which is appropriate in the absence of clear independent variables (Silvestro et al., 2022). We used linear regression models to assess the influence of climatic variables and DBH on xylem phenology.

To determine the optimal sample size for spring and autumn phenology, we conducted 10,000 bootstrap simulations across sampling levels (2–300 trees), recalculating the mean and s.d. for each phenological phase. We calculated the margin of error (ME), which varies across different confidence levels (80%, 90%, 95%, and 99%) due to random sampling, using Eq. 2 (Puth et al., 2015):

$$\mathrm{ME} = t \times \mathrm{s.d.} \quad (2)$$

where t (the critical value) represents the two-tailed *t*-value at the different confidence level with (n – 1) degrees of freedom, and $\mathrm{s.d.}$ is the standard deviation of the bootstrap mean values. We defined the minimum sample size as the smallest sample that satisfies the confidence interval and ME for each phenology phase.

Analysis of variance (ANOVA) and Tukey's honestly significant difference (HSD) tested the difference in phenology, cell production, and duration of each phenology phase between years. All statistical analyses were performed using R version 4.4.0 (R Core Team, 2025).

3 Results

3.1 Individual variability in xylem phenology

On average, cell enlargement began between DOY 153 and 167, wall thickening started between DOY 163 and 180, and cell maturation commenced between DOY 172 and 187. The growth reactivated earlier in 2021 and later in 2019 (Fig. 2). The ending of cell enlargement ranged from DOY 209 to 218. Cell wall thickening ceased between DOY 223 and 238. In autumn, growth ended earlier in 2021 and later in 2018 ($p < 0.05$). Xylem cell production showed a pronounced interannual variability, ranging from 27.4 cells in 2019 to 47.9 cells in 2018 ($p < 0.05$).

In spring, 77%–83% of the plots exhibited phenological phases occurring within a 15-day window, indicating a high degree of temporal clustering across plots (Fig. S1). In contrast, autumn phenology was more heterogeneous, with only 60%–62% of plots showing phases within the same time window. Significant differences in the duration of phenological phases between spring and autumn were also observed (Table 1, $p < 0.05$). In spring, trees in the same plot completed each phenological phase within an average period of 11 days, reflecting a high degree of synchrony among individuals. In autumn, this period ranged from 14 to 22 days, indicating a higher heterogeneity within plots.

3.2 Phenological variability and cell production

Variance component analysis showed that spring phenology was largely driven by temperature and precipitation, which together explained about 70% of the total variance, indicating strong climatic control (Fig. 3). In contrast, autumn phenology was more influenced by plot and DBH, reflecting the greater importance of structural traits and site conditions. To further explore these patterns, we identified key climatic windows based on previous studies and our own observations (Fig. S2). May was the critical month for spring phenology, while July and August were most relevant for the ending

of cell enlargement and wall thickening, respectively (Fig. S3). Spring phenology was significantly correlated with May temperature ($p < 0.001$), confirming their climatic dependence (Fig. S4). In contrast, autumn phenology showed weaker or no correlations with temperature, but was significantly delayed in trees with larger DBH ($p < 0.01$), underscoring the role of tree size in regulating late-season dynamics.

Strong correlations were observed among the phenological phases in spring and autumn (Fig. 4; $p < 0.001$). Cell production was negatively correlated with the timings of spring phenological phases and positively correlated with the phases in autumn ($p < 0.001$), indicating that earlier spring onset and later autumn cessation are associated with increased xylem production. Mantel tests revealed that plots with higher xylem cell production also exhibited greater variability in autumn phenology, suggesting that increased growth may contribute to wider heterogeneity among individuals in the timings of growth cessation ($p < 0.05$).

3.3 Duration of growth phases and cell production

The durations of cell enlargement and wall thickening phases varied significantly among years (Fig. 5). On average, cell enlargement lasted 48–60 days, was shorter in 2019 and longer in 2022. Cell wall thickening ranged from 49 to 68 days, lasting longer in 2018 and shorter in 2019. In all years except 2019, the slope of the relationship between onset and duration was smaller than that of the ending, indicating a stronger influence of autumn phenology on the duration of growth (Figs. 6, S3, and S4, $p < 0.001$). The variations in growth duration were also reflected in differences in xylem cell production. SMA regression also confirmed that longer growth phases were associated with higher cell production (Figs. 7, S5, and S6, $p < 0.001$).

3.4 Sample size variability

The sample sizes estimated for the phenological phases in spring were consistently

lower than those in autumn at the same confidence level and error margin (Tables S1–S4). At the 95% confidence level with a ±3-day error margin, spring phenological phases, such as the first wall-thickening cell, required between 8 and 18 trees, whereas autumn phenological phases, such as the ending of cell wall-thickening, required 17 to 42 trees across years. In general, autumn required two to three times larger samples than spring across all tested error margins in order to obtain good estimations of xylem phenology. Analysis of 805 trees over five years indicated that a sample size of 27 trees provides 95% confidence in estimating xylem phenology with a margin of error of 1 week (Table 2).

4 Discussion

4.1 Individual variability in xylem phenology

This study reveals a marked contrast in xylem phenology between spring and autumnal events, with the latter showing a greater temporal dispersion. Such a contrast suggests distinct underlying regulatory mechanisms. Spring development appears to be primarily controlled by external drivers, particularly the temperatures preceding the growing season (Li et al., 2017; Rossi et al., 2016). Despite substantial interannual variation in May temperatures across the study area, cambial reactivation was tightly synchronized among individuals within each year. This pattern likely reflects a consistent, species-specific thermal threshold for the onset of cambial activity, as reported previously (Zeng et al., 2022; Bogdziewicz et al., 2020). This synchrony was reflected in the coordinated expansion of enlarging and wall-thickening cells across individuals. Nevertheless, interannual variation in the timing of spring onset remained pronounced, demonstrating the high sensitivity of spring phenology to the annual variability in temperature (Zeng et al., 2022).

Compared with spring phenology, autumn phenology is likely to be influenced by a more complex interplay of factors, including the climatic conditions throughout the growing season, photoperiod, tree physiological status, and microsite conditions (Rathgeber et al., 2016; Way and Montgomery, 2015). The pronounced variability in xylem autumn phenology observed in our study is consistent with the high inter-individual dispersion in leaf senescence and late-season soil CO_2 efflux reported in previous research (Harel et al., 2023; Perrin et al., 2017; Cuny et al., 2012). Similar patterns have been observed in other boreal species such as larch and black spruce, where autumnal growth cessation reflects both genetic predisposition and environmental influences (Guo et al., 2022; Rossi and Bousquet, 2014). Internal carbon dynamics and sink limitation may further modulate the onset of dormancy. The absence of a clear, dominant external cue during autumn could explain the weaker synchrony observed among individuals, possibly contributing to the relatively limited focus on this phase in phenological research (Gallinat et al., 2015).

Beyond the environmental influences, the variability in autumn phenology could partly reflect differences in individual growth trajectories accumulated earlier in the growing season. Trees that maintained higher cambial activity during spring and summer tended to extend later xylem formation during autumn, contributing to a broader spread in the timing of growth cessation among individuals (Palombo et al., 2018; Rathgeber et al., 2011). This carry-over effect of cumulative growth explains the marked seasonal contrast in phenological synchrony that we observed in our site. This finding aligns with Zhang et al. (2023), who reported that the factors influencing spring and autumn phenology differ markedly, reinforcing the seasonal asymmetry in regulatory mechanisms. The high synchrony in spring likely results from shared climatic triggers, whereas the variability in autumn may be linked to both differences in the microclimate among permanent plots and the accumulated growth performance of individual trees, resulting in diverging stand-level growth and carbon allocation.

4.2 Productivity gains from asynchronous autumn phenology

Sites with greater individual variability in autumn phenology exhibited higher xylem cell production. This pattern likely reflects differences in the duration of cambial activity among trees, with some individuals having higher growth rates and longer growing seasons. Individuals that maintained cell division longer during summer produced more xylem cells and delayed growth cessation into autumn, thereby contributing to both increased annual xylem production and a wider spread in autumn phenology (Rathgeber et al., 2011). The physiological basis of this pattern lies in extended phases of cell enlargement and wall thickening, which are associated with the number of xylem cells to differentiate (Silvestro et al., 2023). A mismatch in growth cessation across individuals reduces the risk of synchronous exposure to unfavorable events in autumn, thus enhancing the resilience to short-term environmental stress (Tilman et al., 2006). Prolonged cambial activity resulting from higher xylem production may delay the onset of dormancy (Lupi et al., 2010), indicating that enhanced growth comes with physiological trade-offs related to seasonal transitions.

Although an increased growth may enhance carbon sequestration at the stand level, greater inter-individual variation in autumn phenology could introduce ecological trade-offs. As individuals diverge in the timing of late-season transitions, synchrony with the photoperiodic signal may become disrupted. Photoperiod regulates key physiological processes, such as nutrient resorption, cessation of cambial activity, and cold acclimation (Mu et al., 2023). Our analysis showed that trees with larger DBH tended to exhibit later cessation of xylem formation (Fig. S4) and that greater phenological variability in autumn coincided with higher cell production across plots. This suggests that prolonged cambial activity in certain individuals may contribute to both enhanced growth and increased variation in phenological timing. Modeling studies have also shown that mismatches between photoperiod and temperature under warming scenarios can delay dormancy and increase frost risk (Rinne et al., 2018; Maurya and Bhalerao, 2017). Together, these findings indicate that while increased variability in autumn phenology may promote growth in some individuals, it may also reduce synchrony at the stand level. This mismatch could weaken seasonal coordination and ultimately reduce the resilience to environmental stress of trees in cold climates (He et al., 2025; Way and Montgomery, 2015).

4.3 Sampling challenges from autumn phenological variability

The asynchronous nature of autumn phenology, reflected in the dispersed timings of growth cessation among individuals, presents significant challenges for phenological monitoring and the standardization of sampling protocols. These challenges may introduce substantial uncertainty in forest carbon modeling, as the timing of phenological events is closely linked to the process of carbon sequestration (Silvestro et al., 2025; Gallinat et al., 2015). Unlike spring phenology, which is typically characterized by a relatively synchronized onset, autumn phenology exhibits a broader temporal spread. This increased variability complicates efforts to identify representative phenological phases at the stand level and makes it more difficult to accurately assess the duration of growth. One key challenge lies in defining a sampling

window that adequately captures the complete range of growth cessation. If sampling ends too early, late-growing individuals may be excluded, leading to biased estimates of population-level phenological timing and obscuring true interannual variability (Keenan et al., 2014). Moreover, the elevated dispersion of autumn phenology increases the sensitivity of phenological metrics to sample size, amplifying the risk of uncertainty when relying on a limited number of individuals.

Refining sampling strategies in xylem phenology is essential for improving the efficiency, reliability, and generalizability of phenological assessments. Our results show that tree size (DBH) significantly influences autumn phenology. Although small sample sizes (i.e., 3–5 trees per site) are common in earlier studies (Wang et al., 2023; Liu et al., 2019; Rossi et al., 2006b), they are typically accompanied by strict selection criteria, such as choosing trees of similar age and size, to reduce the variability of the sample. This may induce a higher bias if not considered, especially important for autumn phenological traits, which are more sensitive to the structural differences among individuals.

While this selective-sampling approach helps to control unwanted variation, it may not fully capture the natural heterogeneity across the stand. Our findings underscore the value of increasing sample size to better represent phenological variability at the population level. According to our results, sampling 27 trees yields estimates of xylem phenology with 95 percent confidence and a margin of error of about one week. In addition to increasing sample size, extending the observation period is equally important to account for late-growing individuals and ensure that the complete duration of phenological phases is captured. These adjustments are expected to enhance the detection of interannual variability and provide a more robust basis for modeling forest phenology and growth dynamics, but involve higher costs for sample and data collection. The development of remote sensing tools to estimate xylem phenology could contribute to improving the estimations as well as reducing the costs for growth monitoring.

5 Conclusion

This study provides the first quantitative assessment of individual variability in xylem phenology using a dataset based on a wide weekly monitoring of over 800 balsam fir trees across five consecutive years. We identified a marked seasonal asymmetry in phenological synchrony. In particular, the phenological phases in spring, triggered mainly by environmental signals, were more synchronized among individuals than autumn phenology, which is affected by both internal and external drivers. The observed asynchrony in autumn phenology primarily reflects variation in the duration of growth among individuals and is associated with higher wood production. Given the pronounced variability in autumn phenology, our study has assessed a sample size of 27 trees to achieve 95% confidence in estimating xylem phenology with a margin of error of 1 week. Failing to account for the seasonal heterogeneity in growth reactivation and cessation may result in underestimating the dynamics of growth and carbon sequestration into the wood, mainly during the late season in autumn. Our findings highlight the importance of better incorporating both seasonal and individual variability into forest carbon models to improve predictions of boreal forest productivity under current or future climates.

Fundings

This work was funded by the Ministère des Ressources naturelles et des Forêts (project number 112332139 led by Jean-Daniel Sylvain and Guillaume Drolet) and the National Science Foundation for Distinguished Young Scholars of China (42425101). Chunsong Wang received the State Scholarship Funding provided by the China Scholarship Council (202408350075) to conduct this research. **Acknowledgements**

We thank M. Rhéaume, T. Duteil, J. Bergeron, P-Y Mondou-Laperrière, L. Papillon, F. Wiseman, P-L. Déchène, É. Saulnier, K. Theriault, and C. Cloutier for technical work in the field and in the lab, Université Laval for permitting access to the site, and A. Garside for editing the English text.

Authors' contributions

Chunsong Wang: Methodology, visualization, writing—original draft; **Jean-Daniel Sylvain**: Conceptualization, methodology, investigation, funding acquisition, project administration, supervision, writing—review & editing; **Roberto Silvestro**: Methodology, Visualization, Funding acquisition, Writing—review & editing; **Guillaume Drolet**: Conceptualization, Methodology, Investigation, Funding acquisition, Project administration, Writing—review & editing; **Keyan Fang**: Conceptualization, Supervision, Writing—review & editing; **Sergio Rossi**: Conceptualization, Visualization, Funding acquisition, Project administration, Supervision, Writing—review & editing.

Data availability

Data will be made available on request.

Declaration of competing interest

The authors declare that they have no known competing financial interests or personal

relationships that could have appeared to influence the work reported in this paper.

References

Bogdziewicz, M., Szymkowiak, J., Bonal, R., Hacket-Pain, A., Espelta, J.M., Pesendorfer, M., Grewling, L., Kasprzyk, I., Belmonte, J., Kluska, K., De Linares, C., Penuelas, J., Fernandez-Martinez, M., 2020. What drives phenological synchrony? Warm springs advance and desynchronize flowering in oaks. Agric. For. Meteorol. 294, 108140. https://doi.org/10.1016/j.agrformet.2020.108140.

Campioli, M., Marchand, L.J., Zahnd, C., Zuccarini, P., McCormack, M.L., Landuyt, D., Lorer, E., Delpierre, N., Gričar, J., Vitasse, Y., 2024. Environmental sensitivity and impact of climate change on leaf-, wood- and root phenology for the overstory and understory of temperate deciduous forests. Curr. For. Rep. 11, 1. https://doi.org/10.1007/s40725-024-00233-5.

Cuny, H.E., Rathgeber, C.B.K., Lebourgeois, F., Fortin, M., Fournier, M., 2012. Life strategies in intra-annual dynamics of wood formation: Example of three conifer species in a temperate forest in north-east France. Tree Physiol. 32, 612–625. https://doi.org/10.1093/treephys/tps039.

Delpierre, N., Berveiller, D., Granda, E., Dufrêne, E., 2016. Wood phenology, not carbon input, controls the interannual variability of wood growth in a temperate oak forest. New Phytol. 210, 459–470. https://doi.org/10.1111/nph.13771.

FAO, 2022. The state of the world's forests 2022: Forest pathways for green recovery and building inclusive, resilient and sustainable economies. Food and Agriculture Organization of the United Nations, Rome, Italy. https://doi.org/10.4060/cb9360en.

Fu, Y.H., Zhang, X., Piao, S., Hao, F., Geng, X., Vitasse, Y., Zohner, C., Penuelas, J., Janssens, I.A., 2019. Daylength helps temperate deciduous trees to leaf-out at the optimal time. Glob. Change Biol. 25, 2410–2418. https://doi.org/10.1111/gcb.14633.

Gallinat, A.S., Primack, R.B., Wagner, D.L., 2015. Autumn, the neglected season in climate change research. Trends Ecol. Evol. 30, 169–176. https://doi.org/10.1016/j.tree.2015.01.004.

Gill, A.L., Gallinat, A.S., Sanders-DeMott, R., Rigden, A.J., Short Gianotti, D.J., Mantooth, J.A., Templer, P.H., 2015. Changes in autumn senescence in northern hemisphere deciduous trees: A meta-analysis of autumn phenology studies. Ann. Bot. 116, 875–888. https://doi.org/10.1093/aob/mcv055.

Guo, X., Klisz, M., Puchałka, R., Silvestro, R., Faubert, P., Belien, E., Huang, J., Rossi, S., 2022. Common-garden experiment reveals clinal trends of bud phenology in black spruce populations from a latitudinal gradient in the boreal forest. J. Ecol. 110, 1043–1053. https://doi.org/10.1111/1365-2745.13582.

Harel, A., Sylvain, J.-D., Drolet, G., Thiffault, E., Thiffault, N., Tremblay, S., 2023. Fine scale assessment of seasonal, intra-seasonal and spatial dynamics of soil CO_2 effluxes over a balsam fir-dominated perhumid boreal landscape. Agric. For. Meteorol. 335, 109469. https://doi.org/10.1016/j.agrformet.2023.109469.

He, M., Sylvain, J.-D., Silvestro, R., Drolet, G., Arsenault, R., Rossi, S., 2025. Xylogenesis under future climates: Enhanced growth of balsam fir in a warming

boreal forest. Front. Plant Sci. 16, 1563051. https://doi.org/10.3389/fpls.2025.1563051.

IPCC, 2023. Climate change 2023: Synthesis report. In: Lee, H., Romero, J. (Eds.), Contribution of Working Groups I, II and III to the Sixth Assessment Report of the Intergovernmental Panel on Climate Change. Intergovernmental Panel on Climate Change, Geneva, Switzerland. https://doi.org/10.59327/IPCC/AR6-9789291691647.

Keenan, T.F., Gray, J., Friedl, M.A., Toomey, M., Bohrer, G., Hollinger, D.Y., Munger, J.W., O'Keefe, J., Schmid, H.P., Wing, I.S., Yang, B., Richardson, A.D., 2014. Net carbon uptake has increased through warming-induced changes in temperate forest phenology. Nat. Clim. Change 4, 598–604. https://doi.org/10.1038/nclimate2253.

Lagueux, P., Sylvain, J.-D., Drolet, G., Isabelle, P.-E., Leonardini, G., Nadeau, D.F., Anctil, F., 2024. Impacts of forest canopy heterogeneity on plot-scale hydrometeorological variables—Insights from an experiment in the humid boreal forest with the Canadian Land Surface Scheme. Agric. For. Meteorol. 357, 110194. https://doi.org/10.1016/j.agrformet.2024.110194.

Legendre, P., Fortin, M., Borcard, D., 2015. Should the Mantel test be used in spatial analysis? Methods Ecol. Evol. 6, 1239–1245. https://doi.org/10.1111/2041-210X.12425.

Li, X., Liang, E., Gričar, J., Rossi, S., Čufar, K., Ellison, A.M., 2017. Critical minimum temperature limits xylogenesis and maintains treelines on the southeastern Tibetan Plateau. Sci. Bull. 62, 804–812. https://doi.org/10.1016/j.scib.2017.04.025

Liu, X., Wang, C., Zhao, J., 2019. Seasonal drought effects on intra-annual stem growth of Taiwan pine along an elevational gradient in subtropical China. Forests 10, 1128. https://doi.org/10.3390/f10121128.

Liu, Z., Ciais, P., Penuelas, J., Xia, J., Zhou, S., Zhang, Y., Fu, Y.H., 2025. Enhanced vegetation productivity driven primarily by rate not duration of carbon uptake. Nat. Clim. Change https://doi.org/10.1038/s41558-025-02311-3.

Lupi, C., Morin, H., Deslauriers, A., Rossi, S., 2010. Xylem phenology and wood production: Resolving the chicken-or-egg dilemma. Plant Cell Environ. 33, 1721–1730. https://doi.org/10.1111/j.1365-3040.2010.02176.x.

Marchand, L.J., Dox, I., Gričar, J., Prislan, P., Leys, S., Van Den Bulcke, J., Fonti, P., Lange, H., Matthysen, E., Penuelas, J., Zuccarini, P., Campioli, M., 2020. Inter-individual variability in spring phenology of temperate deciduous trees depends on species, tree size and previous year autumn phenology. Agric. For. Meteorol. 290, 108031. https://doi.org/10.1016/j.agrformet.2020.108031.

Mu, W., Wu, X., Camarero, J.J., Fu, Y.H., Huang, J., Li, X., Chen, D., 2023. Photoperiod drives cessation of wood formation in northern conifers. Glob. Ecol. Biogeogr. 32, 603–617. https://doi.org/10.1111/geb.13647.

Maurya, J.P., Bhalerao, R.P., 2017. Photoperiod- and temperature-mediated control of growth cessation and dormancy in trees: A molecular perspective. Ann. Bot. 120, 351–360. https://doi.org/10.1093/aob/mcx061.

514 Palombo, C., Fonti, P., Lasserre, B., Cherubini, P., Marchetti, M., Tognetti, R., 2018.
515 Xylogenesis of compression and opposite wood in mountain pine at a
516 Mediterranean treeline. Ann. For. Sci. 75, 93. https://doi.org/10.1007/s13595-
517 018-0773-z.
518 Perrin, M., Rossi, S., Isabel, N., 2017. Synchronisms between bud and cambium
519 phenology in black spruce: Early-flushing provenances exhibit early xylem
520 formation. Tree Physiol. 37, 593–603. https://doi.org/10.1093/treephys/tpx019.
521 Piao, S., Liu, Q., Chen, A., Janssens, I.A., Fu, Y., Dai, J., Liu, L., Lian, X., Shen, M.,
522 Zhu, X., 2019. Plant phenology and global climate change: Current progresses
523 and challenges. Glob. Change Biol. 25, 1922–1940.
524 https://doi.org/10.1111/gcb.14619.
525 Puth, M., Neuhäuser, M., Ruxton, G.D., 2015. On the variety of methods for
526 calculating confidence intervals by bootstrapping. J. Anim. Ecol. 84, 892–897.
527 https://doi.org/10.1111/1365-2656.12382.
528 Rathgeber, C.B.K., Cuny, H.E., Fonti, P., 2016. Biological basis of tree-ring
529 formation: A crash course. Front. Plant Sci. 7, 734.
530 https://doi.org/10.3389/fpls.2016.00734.
531 Rathgeber, C.B.K., Rossi, S., Bontemps, J.-D., 2011. Cambial activity related to tree
532 size in a mature silver-fir plantation. Ann. Bot. 108, 429–438.
533 https://doi.org/10.1093/aob/mcr168.
534 Richardson, A.D., Keenan, T.F., Migliavacca, M., Ryu, Y., Sonnentag, O., Toomey,
535 M., 2013. Climate change, phenology, and phenological control of vegetation
536 feedbacks to the climate system. Agric. For. Meteorol. 169, 156–173.
537 https://doi.org/10.1016/j.agrformet.2012.09.012.
538 Rossi, S., Anfodillo, T., Čufar, K., Cuny, H.E., Deslauriers, A., Fonti, P., Frank, D.,
539 Gričar, J., Gruber, A., Huang, J., Jyske, T., Kašpar, J., King, G., Krause, C.,
540 Liang, E., Mäkinen, H., Morin, H., Nöjd, P., Oberhuber, W., Treml, V., 2016.
541 Pattern of xylem phenology in conifers of cold ecosystems at the Northern
542 Hemisphere. Glob. Change Biol. 22, 3804–3813.
543 https://doi.org/10.1111/gcb.13317.
544 Rossi, S., Anfodillo, T., Menardi, R., 2006a. Trephor: A new tool for sampling
545 microcores from tree stems. IAWA J. 27, 89–97.
546 https://doi.org/10.1163/22941932-90000139.
547 Rossi, S., Bousquet, J., 2014. The bud break process and its variation among local
548 populations of boreal black spruce. Front. Plant Sci. 5, 574.
549 https://doi.org/10.3389/fpls.2014.00574
550 Rossi, S., Deslauriers, A., Anfodillo, T., 2006b. Assessment of cambial activity and
551 xylogenesis by microsampling tree species: An example at the Alpine timberline.
552 IAWA J. 27, 383–394. https://doi.org/10.1163/22941932-90000161
553 R Core Team, 2025. R: A language and environment for statistical computing. R
554 Foundation for Statistical Computing, Vienna, Austria.
555 Rinne, P.L., Paul, L.K., van der Schoot, C., 2018. Decoupling photo- and
556 thermoperiod by projected climate change perturbs bud development, dormancy
557 establishment and vernalization in the model tree *Populus*. BMC Plant Biol. 18,

220. https://doi.org/10.1186/s12870-018-1414-7.

Silvestro, R., Deslauriers, A., Prislan, P., Rademacher, T., Rezaie, N., Richardson, A.D., Vitasse, Y., Rossi, S., 2025. From roots to leaves: Tree growth phenology in forest ecosystems. Curr. For. Rep. 11, 12. https://doi.org/10.1007/s40725-025-00245-9.

Silvestro, R., Mencuccini, M., García-Valdés, R., Antonucci, S., Arzac, A., Biondi, F., Buttò, V., Camarero, J.J., Campelo, F., Cochard, H., Čufar, K., Cuny, H.E., De Luis, M., Deslauriers, A., Drolet, G., Fonti, M.V., Fonti, P., Giovannelli, A., Gričar, J., Rossi, S., 2024. Partial asynchrony of coniferous forest carbon sources and sinks at the intra-annual time scale. Nat. Commun. 15, 6169. https://doi.org/10.1038/s41467-024-49494-5.

Silvestro, R., Zeng, Q., Buttò, V., Sylvain, J.-D., Drolet, G., Mencuccini, M., Thiffault, N., Yuan, S., Rossi, S., 2023. A longer wood growing season does not lead to higher carbon sequestration. Sci. Rep. 13, 31336. https://doi.org/10.1038/s41598-023-31336-x.

Silvestro, R., Sylvain, J.-D., Drolet, G., Buttò, V., Auger, I., Mencuccini, M., Rossi, S., 2022. Upscaling xylem phenology: Sample size matters. Ann. Bot. 130, 811–824. https://doi.org/10.1093/aob/mcac110.

Tilman, D., Reich, P.B., Knops, J.M.H., 2006. Biodiversity and ecosystem stability in a decade-long grassland experiment. Nature 441, 629–632. https://doi.org/10.1038/nature04742.

Wang, C., Zheng, Z., Zhou, F., Liu, X., Fonti, P., Gao, J., Fang, K., 2023. Intra-annual dynamic of opposite and compression wood formation of *Pinus massoniana* Lamb. in humid subtropical China. Front. For. Glob. Change 6, 1224838. https://doi.org/10.3389/ffgc.2023.1224838.

Way, D.A., Montgomery, R.A., 2015. Photoperiod constraints on tree phenology, performance and migration in a warming world. Plant Cell Environ. 38, 1725–1736. https://doi.org/10.1111/pce.12431.

Zeng, Q., Khan, A., Deslauriers, A., Rossi, S., 2022. May temperature drives cambial resumption in the boreal black spruce. Forests 13, 2168. https://doi.org/10.3390/f13122168.

Zhang, Y., Huang, J.-G., Wang, M., Wang, W., Deslauriers, A., Fonti, P., Liang, E., Mäkinen, H., Oberhuber, W., Rathgeber, C.B.K., Tognetti, R., Treml, V., Yang, B., Zhai, L., Antonucci, S., Buttò, V., Camarero, J.J., Campelo, F., Čufar, K., Rossi, S., 2024. High preseason temperature variability drives convergence of xylem phenology in the Northern Hemisphere conifers. Curr. Biol. 34, 1161–1167.e3. https://doi.org/10.1016/j.cub.2024.01.039.

Zhang, J., Gou, X., Rademacher, T., Wang, L., Li, Y., Sun, Q., Wang, F., Cao, Z. 2023. Interaction of age and elevation on xylogenesis in *Juniperus przewalskii* in a cold and arid region. Agric. For. Meteorol., 337, 109480. https://doi.org/10.1016/j.agrformet.2023.109480.

600

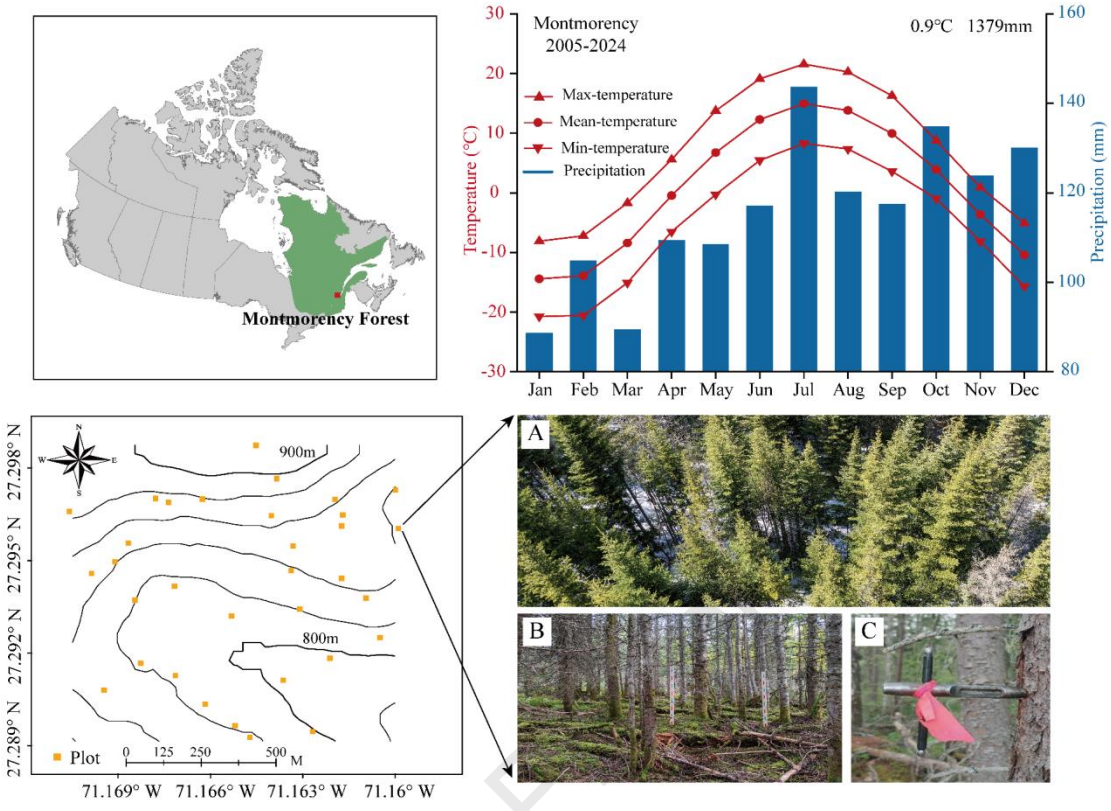

601

602 **Fig. 1.** Map of the sample site in Quebec, Canada. The monthly weather dynamics in
603 Montmorency meteorological station with mean annual temperature and total
604 precipitation in the upper right corner of the upper right panel. Location of the sample
605 plots within the experimental setup in Montmorency Forest (lower left panel). Pictures
606 in the lower right panel show **(a)** an aerial view of a sample plot, **(b)** balsam fir trees
607 within a plot, and **(c)** Trephor tool used for sampling microcores (Credits: L. Papillon,
608 J.-D. Sylvain).

609

610

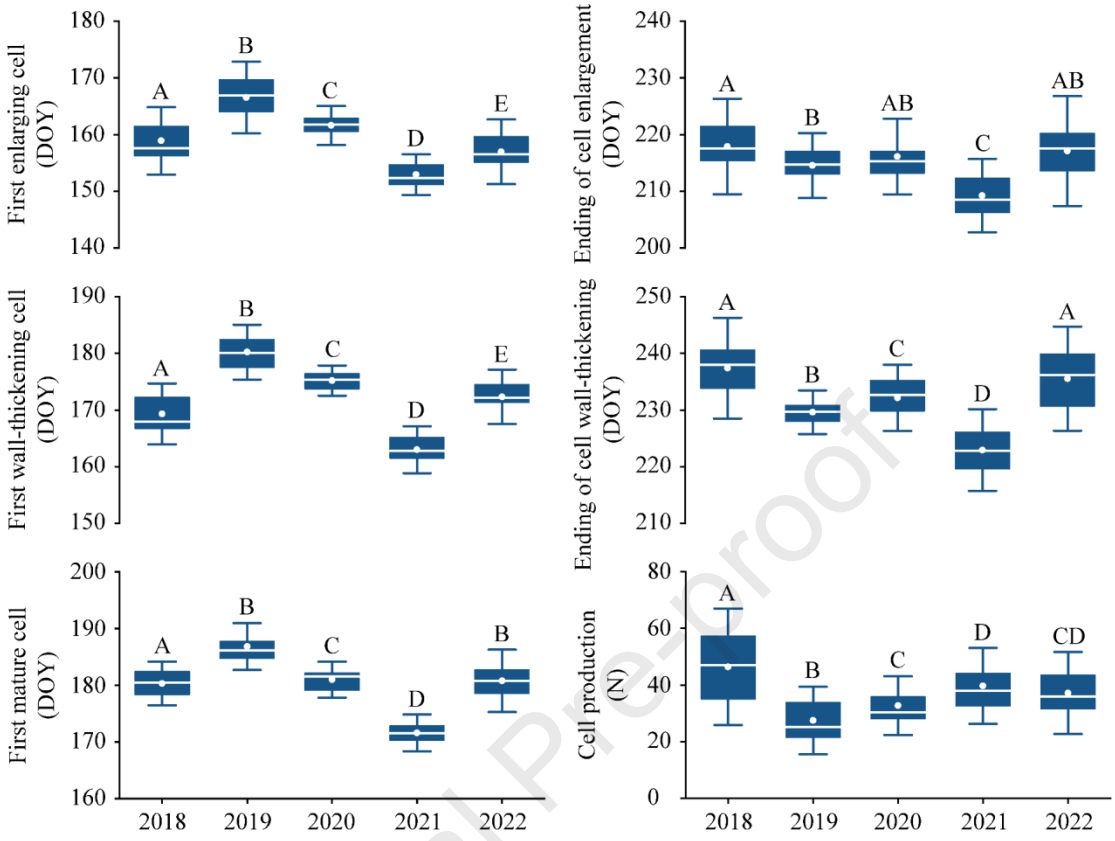

611

612 **Fig. 2.** Phenological and production of xylem variability in balsam fir during 2018–
613 2022. Different letters indicate significant differences between years ($p < 0.05$).
614 Horizontal boxplots represent upper and lower quartiles, white horizontal lines
615 represent median values, and white dots represent mean values.

616

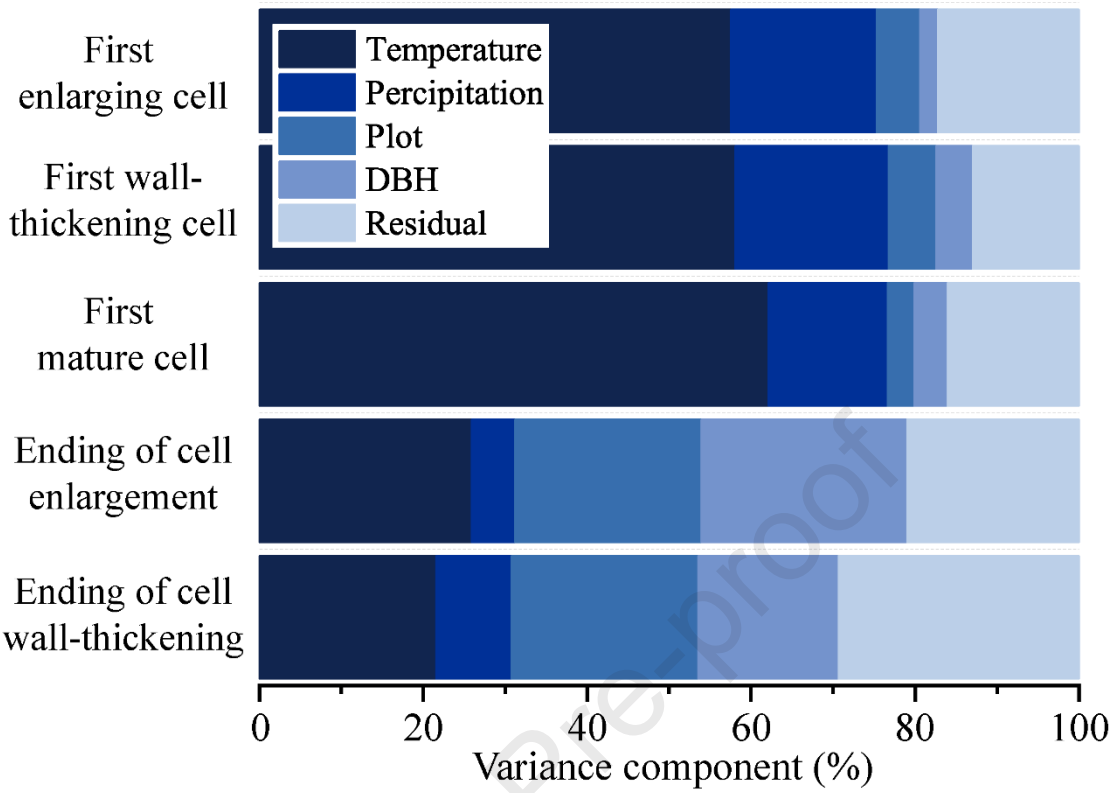

Fig. 3. Components of the variance of xylem phenology in balsam fir between plots. Estimated using linear mixed-effects models.

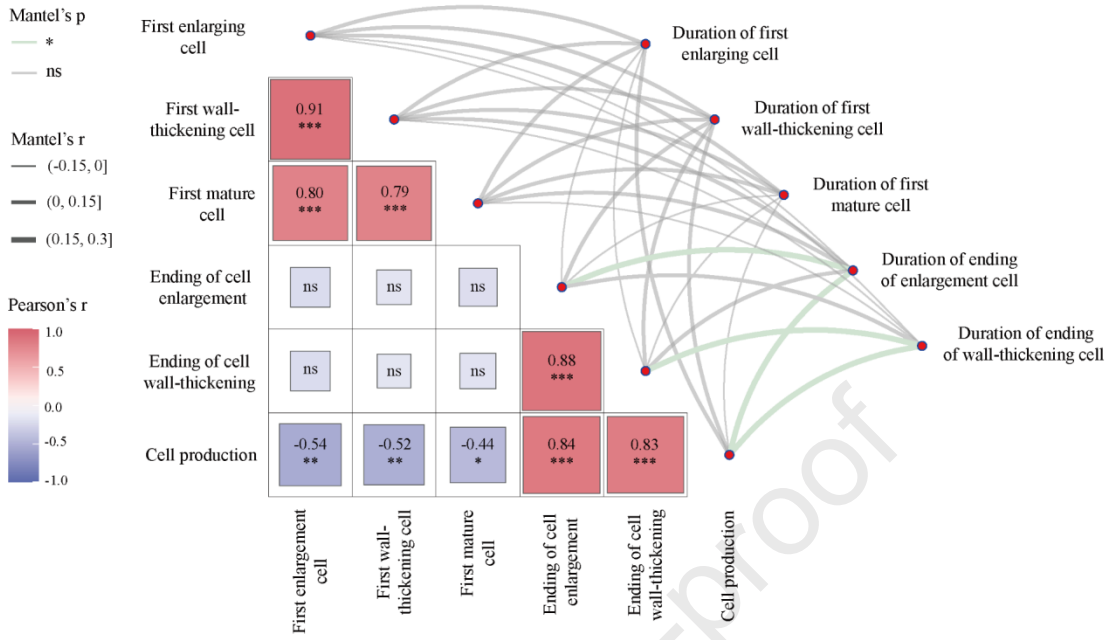

Fig. 4. Pairwise comparisons of xylem phenology and cell production in balsam fir. The left panel shows Pearson correlation coefficients (*r*) between the xylem phenology and cell production. Color gradients range from blue (negative) to red (positive), with * < 0.05, ** < 0.01, *** < 0.001. The right panel displays Mantel test results between the xylem phenology and duration of phenological phase, where edge width is proportional to the Mantel's *r* value and edge color indicates statistical significance (green = $p < 0.05$; grey = ns). Each node represents a variable, and node positions align with those in the correlation matrix.

633

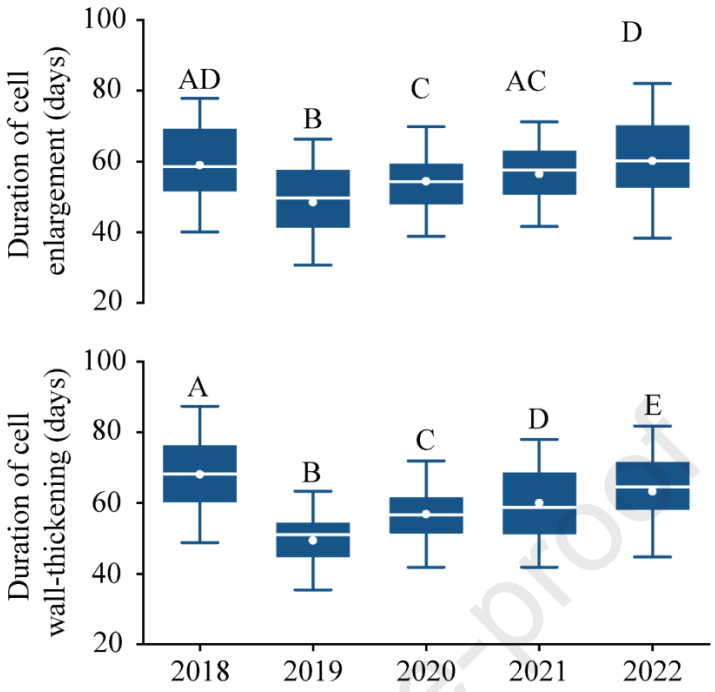

634

635 **Fig. 5.** Duration of enlargement and cell wall-thickening in balsam fir during 2018–
636 2022. Different letters indicate significant differences between years ($p < 0.05$).
637 Horizontal boxplots represent upper and lower quartiles, white horizontal lines
638 represent median values, and white dots represent mean values.

639

640

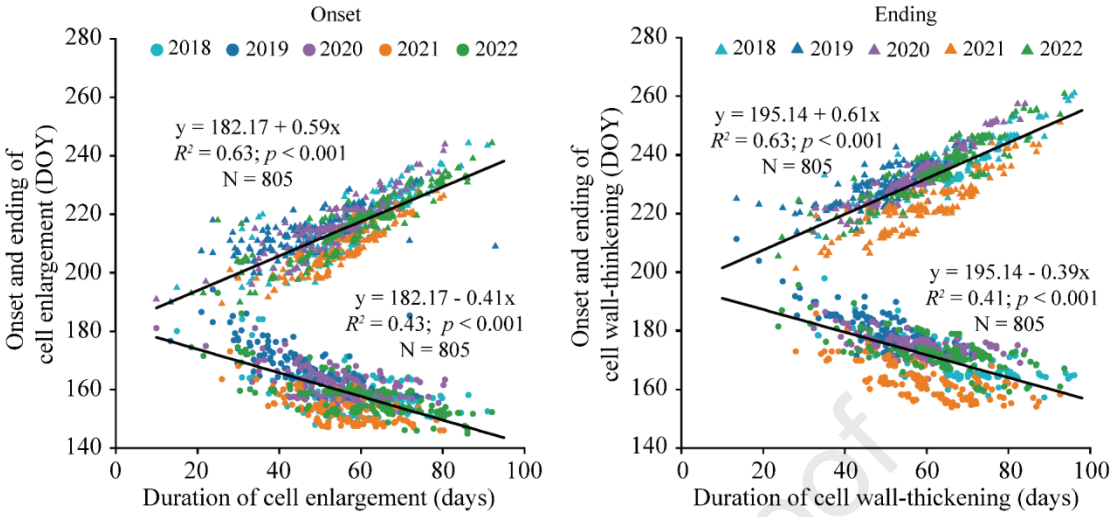

641

642 **Fig. 6.** Sample linear regression timings of onset and ending of cell division and
643 differentiation, and duration of cell division and differentiation of balsam fir during
644 2018–2022.

645

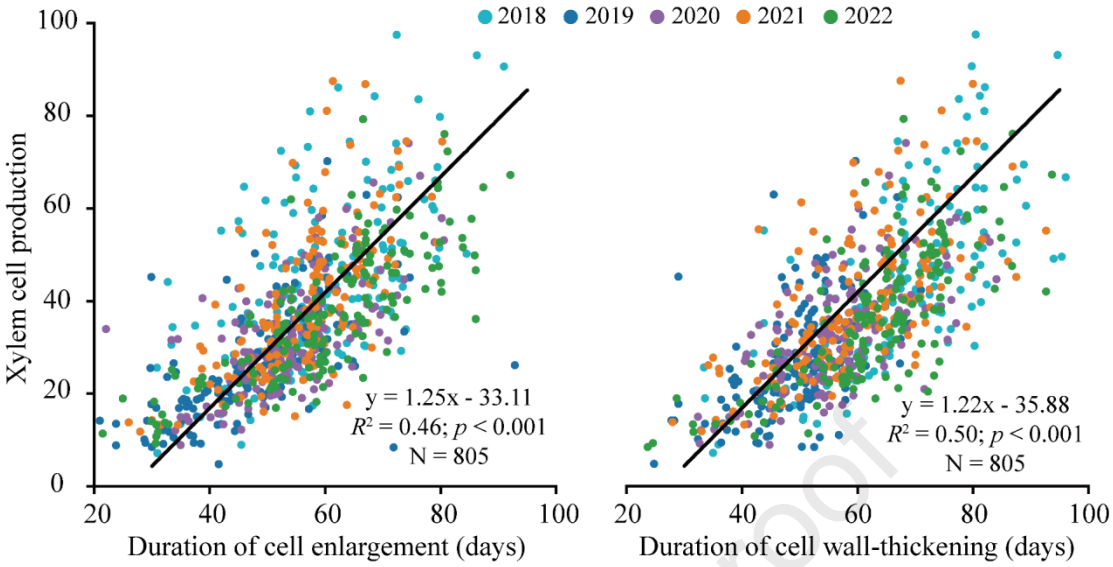

646

647 **Fig. 7.** SMA regression among duration of cell division and differentiation and xylem
648 cell production of balsam fir during 2018–2022.

649

650 **Table 1**

651 Mean duration of different xylem phenological phases between plots in balsam fir.
652 Different letters indicate significant differences between each phenological phase ($p <$
653 0.05)

Phenology	Year				
	2018	2019	2020	2021	2022
First enlarging cell	9.8±5.5^{A}	11.5±5.6^{A}	10.3±4.7^{A}	8.2±4.3^{A}	9.9±5.4^{A}
First wall-thickening cell	10.3±4.8^{A}	10.8±5.4^{A}	7.0±4.1^{A}	12.2±4.2^{A}	8.6±4.7^{A}
First mature cell	10.2±4.8^{A}	7.2±5.2^{A}	6.9±5.1^{A}	8.4±4.0^{A}	10.6±5.3^{A}
Ending of cell enlargement	22.1±8.9^{B}	13.7±5.6^{B}	18.4±7.7^{B}	16.0±6.2^{B}	20.2±8.6^{B}
Ending of cell wall-thickening	18.5±9.6^{C}	13.4±5.9^{B}	19.8±8.6^{B}	17.7±9.4^{B}	17.1±7.2^{B}

654

655 **Table 2**

656 Minimum sample size for each phenological phase for 95% confidence level at different
657 margins of error (±1, ±2, ±3, and ±4)

Phenology	Margin of error (± days)			
	± 1	**± 2**	**± 3**	**± 4**
First enlarging cell	232	61	29	17
First wall-thickening cell	241	62	30	18
First mature cell	185	50	24	15
End of cell enlargement	341	88	40	24
End of cell wall-thickening	387	98	45	27
Average	277	71	34	20

658

659

Declaration of interests

☒ The authors declare that they have no known competing financial interests or personal relationships that could have appeared to influence the work reported in this paper.

☐ The authors declare the following financial interests/personal relationships which may be considered as potential competing interests: